The Sun and Space Weather

Arnold Hanslmeier

1 Definition of Space Weather and Some Examples

1.1 Definition

The US National Space Weather Programme gave the following definition of Space Weather:

Conditions on the Sun and in the solar wind, magnetosphere, ionosphere and thermosphere that can influence the performance and reliability of space-borne and ground-based technological systems and can endanger human life or health.

This definition can be extended to:

All influences on Earth and near Earth's space.

Space Weather plays an important role in modern society since we strongly depend on communication which is mostly based on satellites and thus influenced by the propagation of signal throughout the atmosphere. Moreover, satellites themselves are vulnerable to space weather:

- Space Shuttle: numerous micrometeoroid/debris impacts have been reported.
- Ulysses: failed during peak of Perseid meteoroid shower.
- Pioneer Venus: Several command memory anomalies related during high-energy cosmic rays.
- GPS satellites: photochemically deposited contamination on solar arrays.
- 1989 power failure in Quebec due to magnetic storms.
- On Earth: radio fadeouts. The HF communication depends on the reflection of signals in the upper Earth's atmosphere $\Leftarrow$ strongly influenced by the Sun's shortwave radiation.

An introduction to space weather with much more references was given by Hanslmeier, 2007.

Arnold Hanslmeier
Institute of Physics, Dep. of Geophysics, Astrophysics and Meteorology, Univ.-Platz 5, A-8010 Graz, Austria, e-mail: arnold.hanslmeier@uni-graz.at

The short term effects are summarized as `space weather` but also long term effects have to be taken into consideration: the solar luminosity has evolved from about 75 percent four billion years ago to its present value and will slightly increase in the future. The galactic environment changes due the rotation of the solar system around the galactic center. These long term effects are summarized as `space climate`.

The Sun including interactions between solar magnetosphere and solar wind with the Earth's magnetosphere is the main driver for space weather but also other sources like space debris, asteroids, meteoroids, radiation and particles, cosmic rays, nearby supernova explosions and even the galactic environment are to be included in this definition.

1.2 Space Weather Costumers

Modern communication systems, based on Earth or on satellites as well as power systems on Earth and health of astronauts can be strongly influenced by space weather. Therefore, the aim of space weather research is to try to avoid negative consequences, mainly by efficient system design and warning.

Costumers of space weather predictions are satellite designers and operators, manned space flight missions, telecommunication companies and power suppliers.

One of the main aims of solar research is to understand better the mechanisms that produce space weather relevant phenomena on the Sun (like flares or CMEs) and to predict the occurrence of energetic solar events that influence on space weather.

There are many organizations throughout the world which are strongly devoted to space weather research, for example the US Space Weather Program, US-NASA's Living With a Star program, ESA's space weather program, SWENET, Space Weather European Network, SIDC, Solar influences data center at the Royal Observatory in Belgium, Lund space weather center, the Australian IPS Radio and Space Services , the Australian Space Weather Agency, and many others (such as the Group in Oulu, Finland).

2 Some MHD Basics

In this chapter we shortly review basic equations from MHD in order to understand the complex interactions that occur during flaring processes on the Sun or when solar magnetic fields and particles interact with the geomagnetic field.

2.1 The Lorentz Force

Magnetic fields are generated by currents (flow of charged particles) and changing electric fields. There are always magnetic dipoles. The `Lorentz force` is the force on a point charge q due to electromagnetic fields. Considering only a magnetic field B, the Lorentz force is given by:

$$\mathbf{F} = q(\mathbf{v} \times \mathbf{B}) \tag{1}$$

F in Newtons, q in Coulombs, **v** in m/s, **B** in Teslas.

In the general Lorentz equation the electric field **E** enters as

$$m\frac{d\mathbf{v}}{dt} = q(\mathbf{E} + \mathbf{v} \times \mathbf{B}) \tag{2}$$

and the Lorentz force can be split into components of motion normal and parallel to the magnetic field.

2.2 Charged particles and fields

Consider a magnetic field line and a charged particle. In case of equilibrium between centrifugal force and Lorentz force we can derive the radius of gyration, r:

$$\frac{mv^2}{r} = qvB \qquad r = \frac{mv}{qB} \tag{3}$$

Therefore, charged particles circulate around magnetic field lines and the sense of rotation is clockwise for negative particles. More generally, motion is circular about an imaginative guiding center. The Gyrofrequency or Larmorfrequency is given by:

$$\omega = \frac{qB}{m} \tag{4}$$

in rad/s.

Example: Radius of gyration in Earth's magnetosphere; consider a particle: e^- with 100 keV, $E = mv^2/2$; its radius of gyration is 100 m.

Under the action of some external force, **F**, a drift of particles occurs, the `drift velocity` is given by:

$$\mathbf{v}_{\mathrm{df}} = c\frac{\mathbf{F} \times \mathbf{B}}{q\mathbf{B}^2} \tag{5}$$

As an example we consider the gradient of the magnetic field around a planet which occurs since the field strength decreases with increasing distance.

$$\mathbf{F} = -\mu_b \nabla B \tag{6}$$

This force produces a drift velocity, electrons and protons drift in opposite directions the electrons eastwards. Therefore, a ring current system develops which strengthens the field in the outside more towards the Sun.

Other examples are the field curvature drift, the gravitational field drift, the electrical field drift

$$\mathbf{F} = q\mathbf{E} \tag{7}$$

here the drift velocity becomes:

$$\mathbf{v}_E = \frac{c\mathbf{E} \times \mathbf{B}}{B^2} \tag{8}$$

Particles move perpendicular to **E** and **B** and protons and electrons move in the same direction. The $\nabla\mathbf{B}$, $\mathbf{E} \times \mathbf{B}$ drift dominate in magnetosphere!

2.3 Magnetic mirror

What happens if the field strength changes along the motion of a particle? The particles are bounced back from the strong field strength region. In the magnetosphere, electrons and ions will bounce back and forth between the stronger fields at the poles. $B_{\max}$, $B_{\min}$ denote the maximum and minimum field strengths and particles with a pitch angle greater than:

$$(v_\perp / v_\parallel)_{\text{crit}} = \sqrt{B_{\max}/B_{\min} - 1} \tag{9}$$

will be reflected!

Note also, that charged particles cannot penetrate magnetic field lines. Therefore, the magnetic field of the Earth provides a shielding against charged particles (mainly coming from the Sun).

2.4 The Earth's magnetic field

The geomagnetic field can be characterized as non static with a field strength between 30 microteslas to 60 microtelsas (at the poles). Close to the poles, the geomagnetic field appears as unipolar (like the gravitational field) and its strength varies as $\sim r^{-2}$, far from the poles it behaves like a dipole $\sim r^{-3}$. The K-index describes its long term stability.

The shape of the geomagnetic field is strongly influenced by the interaction with the interplanetary magnetic field, IMF, and the solar wind particles. The `magnetopause` is the region which is defined by the equality of solar wind pressure and magnetic pressure. Reconnection occurs when the interplanetary magnetic field, IMF, is antiparallel to the Earth magnetic field. The particles become thermalized in the region between the bow shock and the magnetopause. Shocks occur

when something is travelling faster that the local speed of sound and properties like density, pressure, velocity change almost instantaneously. In the `bow shock`, supersonic solar particles hit the magnetosphere.

Both the Alfvén- and the sound velocity are supersonic (Machnumber >1).

$$v_A = \frac{B}{\sqrt{\mu_0 \rho}} \qquad v_s = \sqrt{\frac{c_p}{c_v}\frac{p}{\rho}} \tag{10}$$

The solar wind stretches the dipole field, compressing it on the side toward the Sun and stretching it into a long tail where the field lines close at very long distances ($\sim 3000 R_E$, R_E Earth's radius).

The `plasmasheet` is a sheet of plasma in the tail region dividing the two lobes of the Earth's magnetic field. For both electrons and protons the particle density is 0.5 cm^{-3}. The Lobes are in the `magnetotail` having opposite direction and separated by the plasmasheet - otherwise they would cancel. The `plasmasphere` is a torus shaped region, surrounding the Earth. It was detected in 1963 and has a very sharp edge at the `plasmapause` extending to 4-6 Earth radii, down to the ionosphere. Inside the plasmapause geomagnetic field lines rotate with the Earth. Outside the plasmasphere, magnetic field lines are unable to corotate, the solar wind influence is too large. The plasmasphere is mainly composed of hydrogen.

The `Van Allen radiation belts` were discovered in 1958 by Van Allen; like the plasmasphere they are toroidally shaped. The outer belt extends from 5 to 10 Earth-radii, R_E, the particles are found in the energy range between 0.1 to 10 MeV the inner belt from 0.1 to 1.5 R_E 100 MeV

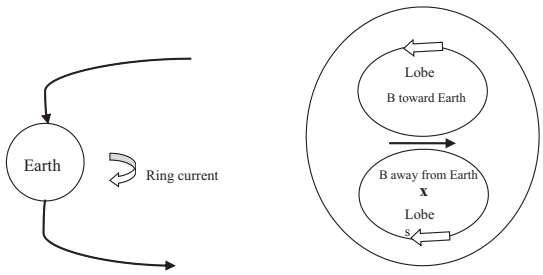

Fig. 1 Global structure of the Earth's magnetic field. In the two lobes the field is opposite and the lobes are separated by a plasmasheet. For the southern half of the magnetosphere the current is clockwise. In the middle both systems add to form a neutral sheet. The right drawing is a cross section of the left at a distance of 20 r_E.

The variations of the geomagnetic field can be classified into short term variations caused e.g. by flares, geomagnetic storms, and long term variations (some quasi-periodicity of 250 000 years). When the interplanetary magnetic field, IMF, has a southward oriented component ($B_z < 0$), reconnection occurs i.e. the field lines

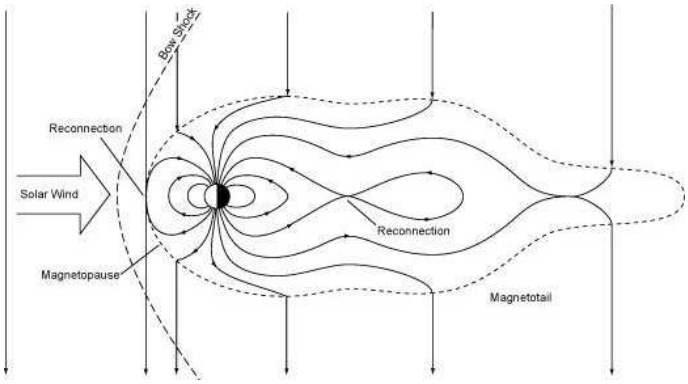

Fig. 2 Reconnection in the bow shock region of the geomagnetic field.

of the IMF cancel with those of the geomagnetic field. Reconnection can also occur in the magnetotail by compressing that region during strongly enhanced flow of particles. When the field is cancelled by reconnection, charged particles can penetrate. Therefore, the number of particles increases because from reconnection at the magnetopause and reconnection in the tail.

Yermolaev *et al.*, 2005, reviewed geomagnetic storm effectiveness of CMEs and solar flares.

3 Solar Energetic Phenomena

We overview briefly the most relevant phenomena on the Sun for space weather. More details can be found in other chapters of this book.

3.1 Active Regions

Big `sunspots` can be even seen with the naked eye on the solar disk and were already known to the ancients. Sunspots are dark spots associated with magnetic field that inhibit convective energy transport and thus cool them. They consist of a dark umbra at a temperature T $\sim$ 4 500 K which is less than in the photosphere (T$\sim$ 6 000 K). More than 150 years ago it was found that their number varies with a period of about eleven years. This sunspot cycle is nowadays called `solar activity cycle` because all energetic phenomena on the Sun vary with this cycle (at least their occurrence).

The solar irradiance is reduced by about 0.02% when a large spot group passes over the Sun. However, this sunspot deficit is overcompensated by `faculae` that are brighter and hotter regions often in the vicinity of spots. In the photosphere

they are seen near the solar limb. Faculae can be observed on the whole disk using filtergrams (observation of the sun at a particular wavelength).

An `active region` can be defined as the region where magnetic flux penetrates through the photosphere, therefore spots often appear as a bipolar group. From the photosphere, magnetic fields propagate to the above lying chromosphere and corona, with expanding field lines. In the photosphere, because of the larger density, plasma motions drill the magnetic field lines that are said to be frozen in. Because of the motions of their footpoints in the photosphere, higher in the chromosphere and corona the field lines can reconnect and magnetic energy is released. This gives rise to a solar flare.

3.2 Flares and CMEs

`Flares` occur in the corona and produce X-rays and UV-radiation which indicates high temperatures and energies during a flare outburst. Also energetic particles are emitted and a small fraction is accelerated to high energies and synchrotron radiation, produced by electrons moving in helical paths around magnetic field lines, is generated (this can be observed as `bursts` in the radio part of the electromagnetic spectrum). During an intense flare, the flux of high energetic particles and cosmic rays is increased at the Earth. Magnetic storms on Earth, caused by the compression of the Earth's magnetosphere due to solar energetic particles (SEPs) and the expanding interplanetary magnetic field often occur with a delay of about 36 h after the flaring event was observed on the Sun. Flares occur in regions where there is a rapid change in the direction of the local magnetic field and their energy is a consequence of magnetic reconnection.

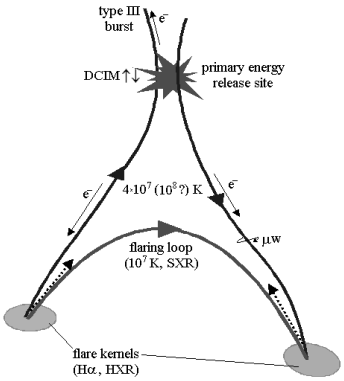

Fig. 3 Two oppositely magnetic field lines interact due to a compression - reconnection occurs - and the resulting flaring loop is shown by bold arrow-lines (grey). Electron beams are marked by e^-, Chromospheric evaporation from the flare kernels is indicated by thick dotted arrows. The primary energy release occurs in the corona at heights between 10^4 and 10^5 km. DCIM indicates fast drifting bursts in the 200-2000 MHz range. HXR (Hard X-ray) emission is related to radio features. HXR emission at successively lower energies indicates delays of slower electrons relative to faster ones. Courtesy: B. Vrsnak.

The power of flares is related to the height of the energy release site. Flares are more powerful and impulsive when the energy release site is located at low heights. This can be explained by the weakening of the magnetic fields with height.

Flares can be classified either by their area on the disk (importance class, see Table 1) or by their soft X-ray emission based on soft X-ray observations of the Sun in the wavelength range 0.1 to 0.8 nm as the peak measured in power of 10 $\mathrm{W\,m^{-2}}$

Table 1 Optical and X-ray classification scheme of solar flares.

Importance class	Area A at disk 10^{-6} sol. hemisphere	Energy (erg)	SXR class	Energy 0.1-.8 nm
S	A<100	10^{28}	A	-8
1	$100 \leq A < 250$	10^{29}	B	-7
2	$250 \leq A < 600$	10^{30}	C	-6
3	$600 \leq A < 1200$	10^{31}	M	-5
4	$A \geq 1200$	10^{32}	X	-4

Example: a B5 flare has a peak flux of $5 \times 10^{-7}\,\mathrm{Wm^{-2}}$. Flares smaller than C1 can only be detected during a solar minimum phase when the general X-ray background is low. Occasionally, flares exceed class X9 in intensity and are referred simply to as X10, X11...

Physical processes of particle acceleration, injection, propagation, trapping, and energy loss in solar flare conditions are reviewed by Aschwanden, 2002.

`CME, Coronal mass ejections`, are linked to long duration flares but recent observations also showed that some short duration flares may have ejecta with speeds up to 2 000 km/s. In CMEs the coronal magnetic field lines are opened in eruptive events. There occurs a closing down or reconnection within several hours $\rightarrow$ prolonged energy release (typical for gradual or eruptive flares). During solar activity minimum about $\sim$0.5 CMEs $\mathrm{day^{-1}}$ and during solar activity maximum ~ 4.5 $\mathrm{day^{-1}}$ are observed. The CME-mass shows no cycle dependence, during minimum CMEs are concentrated around the equator, during maximum they originate from a wide range of latitudes.

The SECCHI instruments on each of the two STEREO spacecraft are observing Coronal Mass Ejections (CMEs) from their initiation, through the corona, and into interplanetary space beyond the Earth's orbit. Extreme solar winds that are caused by CMEs produce geomagnetic storms and ionospheric storms. Type II bursts are associated with shock acceleration of particles in very fast and wide CMEs and can be used as a proxy for them. Gopalswamy *et al.*, 2005, found that the majority (78 %) of the m-to-km type II bursts were associated with solar energetic particle (SEP) events.

3.3 Solar Wind and Interplanetary Magnetic Field

The `solar wind` is a stream of charged particles expelled from the corona and it varies in strength through the solar activity cycle. The particles arrive at the orbit of Earth at an average speed of about 400 km/s. The total mass loss is a few $10^{-14}\,M_\odot/\mathrm{yr}$. The charged particles flow along the open field lines[1] which are cospatial with coronal holes that are regions of lower density and temperature in the corona.

If the solar wind mass loss was constant over the solar evolution the total mass loss of the Sun over that period would be in the order of $10^{-4}\,M_\odot$.

`Interplanetary Magnetic Field, IMF`: as the Sun rotates these various streams rotate as well (co-rotation) and produce a pattern in the solar wind much like that of a rotating lawn sprinkler. At the orbit of the Earth, one astronomical unit (AU) or about $1.5\times10^8\,\mathrm{km}$ from the Sun, the interplanetary magnetic field makes an angle of about 45 degrees to the radial direction. Further out[2] the field is nearly transverse (i.e. about 90 degrees) to the radial direction.

The Sun's magnetic field, that is carried out into interplanetary space is called the interplanetary magnetic field, IMF. When the orientation of the IMF is antiparallel to the Earth's magnetic field, the disturbances are enhanced because of reconnection.

The whole solar system is embedded in the `heliosphere`. The extension is determined by solar activity.

4 Solar Radiation and Particles

In this chapter we review shortly the effect of solar radiation and particles on space weather.

4.1 Solar Irradiance

The Solar constant S is the amount of the Sun's incoming electromagnetic radiation (Solar radiation) per unit area, measured on the outer surface of Earth's atmosphere.

$$S = 1.36\,\mathrm{Wm}^{-2} \tag{11}$$

The solar irradiance is $1/4S$ because the cross section of the Earth is πr^2 and the energy is distributed over the entire surface $4\pi r^2$. The total solar irradiance, TSI, is monitored from space since 25 years. The solar irradiance is variable due to dark sunspots and bright faculae. Over the cycle 22 the value ranged roughly from 1366.0

[1] The term open magnetic field lines does not imply magnetic monopoles but means that they are closed very far from the Sun in the interplanetary space.

[2] At the orbit of Saturn.

to 1367.5, the cycle 23 had a similar maximum (Mekaoui, De Witte, 2008). Fröhlich (2006) gave an overview of solar irradiance measurements since 1978.

About half of the solar radiation is in the visible, the other half is in the IR, only a very small fraction is in the UV and at shorter wavelength or in the radio.

4.2 Solar Energetic Radiation

The solar radiation varies with (i) the 11 years solar activity cycle and (ii) when large active regions pass over the disk due to the solar rotation. The variation is up to 0.003 in the visible part of the spectrum but strongly increases towards shorter wavelengths. The variation of solar constant between cycle 21 and 22 was 0.1%. Because of this variation, the globally averaged equilibrium surface temperature on the Earth's surface varied about 0.2^0 C.

Table 2 Effects of Solar Radiation at different wavelengths on the Middle and Upper Atmosphere. Variab denotes the variability of the wavelength range.

Wavelength range [nm]	Variab. middle Atm.	Variab. upper Atm.	Effect	Height [km]
1–10, SXR		sporadic	Ion. all	70–100
10–100, XUV	2ppm	2 x	Ion. N_2, O, O_2	
100–120, EUV	6 ppm	30%	Ion. NO	80–100
120–200, VUV	150 ppm	10%	Diss. O_2	40–130
200–240, UV	0.12%	5%	Diss. O_2, O_3	20–40
240–300, UV	1.0%	$<$1%	Diss. O_3	20–40

Solar radiation shortward 320 nm represents only 2% of the total solar irradiance; 0.01% of the incident flux is absorbed in the thermosphere at about 80 km and 0.2% in the stratosphere above 50 km. It controls the thermal structure and photochemical processes above the troposphere; for example the stratosphere is controlled by absorption and dissociation of O_2 in the 175 to 240 nm range. The 205 to 295 nm range is predominantly absorbed by ozone O_3.

The influence of solar radiation is larger for shorter wavelengths that are absorbed higher in the atmosphere: the exospheric temperature changes from about 700 K (solar minimum) to 1200-1500 K (solar maximum).

4.3 Particles

The particle population in the Earth's atmosphere is maintained by three main contributions:

- Electrons: they reach the high latitude thermosphere after interaction with the geomagnetic field and acceleration;
- High energy solar protons: their flux is enhanced during periods of large flares;
- Galactic cosmic rays: they originate from outside the heliosphere but their input on Earth is partly controlled by solar activity.

During large flares, intense fluxes of energetic protons (10...10^4 MeV) penetrate the Earth's polar cap regions, ionization between 100 and 20 km is increased and can last for a few hours to a few days. Large numbers of NO_x molecules are produced leading to a subsequent ozone depletion.

There are hints that the Earth's cloud cover follows the variation in galactic cosmic rays, GCR. The number of these particles hitting the Earth's atmosphere is modulated by the strength of solar activity - the strength of the IMF and solar wind. Cosmogenic isotopes such as ^{14}C are anticorrelated with solar activity. During solar maximum less GCR reach the Earth because of the stronger shielding by the heliosphere. These GCR and the secondary particles they produce may act as condensation nuclei (a recent study was made by Arnold, 2006). A variation in cloud cover of 3 % during an average 11-year solar cycle could have an effect of 0.8–1.7 W/m^2. Besides other influences (e.g. change of the Earth's orbit) the well known different periods of warm and cold climate on Earth can also be explained by long term variation of solar activity. Between 1645 and 1715 the Little Ice Age occurred which coincided with almost no solar activity. During that period the production of the cosmogenic isotope ^{14}C was enhanced.

4.4 Space climate

Table 3 summarizes the effect of different factors on the Earth's climate. As we

Table 3 Various influences on the climate

S, solar constant (at 1 AU)	1360 W/m^2
S/4, top of atmosphere	340 W/m^2
S/4(1-a), a=0.3 Earth's albedo	235 W/m^2
1 % change in the albedo	1 W/m^2
estimated rad. effect due to CO_2 increase since 1750	1.5 W/m^2
doubling of CO_2	4 W/m^2
radiative effect of clouds (cooling)	17-35 W/m^2

have demonstrated, the variation of the solar irradiance is low at least in the course of a solar activity cycle. Solar activity however influences on the flux of cosmic ray particles (GCR) which may act as condensation nuclei for clouds (Svensmark, Friis-Christensen, 1997)

A reconstruction of the climate (e.g. by analysis of fossil pollen, cosmogenic isotopes ($^{16}O/^{18}O$, ^{14}C) shows that several periods of warmth and cold have occurred.

- In the Medieval from $\sim$ 9th to 14th centuries a period of warmth.
- Little Ice Age for the northern hemisphere from 15th to 19th centuries.
- Mid-Holocene warm Period (approx. 6 000 years ago); this seems to be in connection with changes of the Earth's orbit (Theory of Milankovich).
- Penultimate interglacial period (approx. 125 000 years ago). It appears that temperatures (at least summer temperatures) were slightly warmer than today (by about 1 to 2^0 C), caused again by the changes in the Earth's orbit (Hughes and Diaz, 1994).
- Mid-Cretaceous Period (approx. 120-90 million years ago): Breadfruit trees apparently grew as far north as Greenland (55^0 N), and in the oceans, warm water corals grew farther away from the equator in both hemispheres.

It is clear that there exist other than solar influences however, solar variations on the long term certainly influence on the climate.

During its main sequence evolution the Sun has become more luminous:

$$L(t) = [1 + 0.4(1 - t/t_0)]^{-1} L_0 \tag{12}$$

In this formula L_0 is the present solar luminosity and t_0 the present age of the Sun (4.6 Gyr). The early Sun had only 70 % of its present luminosity but was more active. This is also called the faint young Sun problem. Because of this low solar luminosity, the Earth would have been totally covered with ice which would have increased the albedo and therefore the ice would never have melted. There are also strong indications of liquid water present on Mars several 10^8 years ago. Thus there must have been other mechanisms to keep these planets at higher surface temperature, e.g. a higher concentration of greenhouse gases like CO_2 in the primitive Earth atmosphere.

All calculations show that during the early life of the Sun, the UV flux was much higher than today. The early Sun was similar to a T Tauri star. At the age of about 40 million years the Sun became a Main sequence star.

5 Space Weather and Damage

5.1 Effects of radiation on biological systems

The passage of ionizing radiation in a living organisms can result in direct effect on DNA leading to single strand breaks (SSB), double strand breaks (DSB), associated base damage (BD), or clusters of these damage types. Water in the body tends to absorb a large fraction of radiation and becomes ionized forming highly reactive molecules which are called free radicals. Those react with and damage the DNA molecules.

Typical effects of radiation sickness are severe burns that are slow to heal, sterilization, cancer.

To minimize the risk for astronauts and people involved with radiation in general, the US National Council on Radiation Protection and Measurements has established radiation dose limits. For a comparison a computed tomography (CT) of the body corresponds to 10 mSv which is comparable to the annual average background radiation for three years.

Table 4 Radiation dose limits in mSv for astronauts

Time period	blood forming organs	eyes	skin
30 days	250	1000	1500
annual	500	2000	3000
career for males	2000 mSv+75(age[years]-30)	4000	6000
career for females	2000 mSv+75(age[years]-38)	4000	6000

The radiation dose limits for ordinary citizens are much lower (see Table 5). The annual dose is about 50 mSv, the lifetime dose is age [years] x 10 mSv. In the US the total average annual dose is about 3.6 mSv.

Table 5 Total average annual radiation does in the US

radon in the air	2 mSv (56%)
rocks, building material	0.28 mSv (8%)
cosmic rays	0.28 mSv (8%)
natural radioactive material in body	0.39mSv (11%)
medical and dental rays	0.39 mSv (11%)
nuclear medicine tests	0.14 mSv (4%)

Table 6 Single dose effects

0.001 mSv	dental x rays
0.002 mSv	5 hr transcontinental flight
0.02 mSv	chest X-ray
1.000 mSv	radiation sickness
2500 mSv	sterility in females
3500 mSv	sterility in males
4000 mSv	average lethal dose (without any treatment)

5.2 Surface Charging

Explosive Solar Particle events (SPE) are usually associated with solar flares and coronal mass ejections. Protons and electrons are emitted at high velocities which can cause problems in orbiting satellites. In January 1994 three geostationary satellites suffered failures of their momentum wheel control circuity under the influence of the long duration of high energy electron fluxes associated with high speed solar wind streams. Such events may occur also during times of sunspot minimum. The strength of shocks plays a key role in shock-related phenomena, such as radio bursts and solar energetic particle (SEP) generation and this is discussed by Shen *et al.*, 2007.

According to USAF: Damaging conditions are assumed when the daily electron flux (which is given by the number of high energy electrons ($>$ 2MeV) per cm^2 per sterad per day) meets either of the following conditions[3]: greater than 3×10^8 per day for 3 consecutive days; or greater than 10^9 for a single day. Such conditions often occur about 2 days after the onset of a large geomagnetic storm.

The K-index is a measure for geomagnetic storms. The values of K (3 hourly measure) range from 0-9. K=0 means quiet; K$\geq$ 4 surface charging effects could begin, K$\geq$ 6 surface charging is probable. Surface charging usually does not cause big problems, particles with energy $\geq$1 MeV cause Deep Dielectric Charging.

Single-event upsets (SEUs) are random errors in semiconductor memory that occur at a much higher rate in space than on the ground. They are non-destructive, but can cause a loss of data if left uncorrected. SEUs are often associated with heavy ions from the galactic cosmic radiation.

Because of a miss-alignment of the radiation belts (tilt of magnetic axis to rotation axis) in the South Atlantic Anomaly the Earth's surface magnetic field is weakest there. Particles drifting around the Earth travel much closer to the Earth than at other latitudes and longitudes.

A list of different geomagnetic indices which measure the state of the magnetosphere/ionosphere system is given in Table 7.

5.3 Solar Activity and Satellite Lifetimes

Satellites in low Earth orbit (LEO), with perigee altitudes below 2000 km, are subject to atmospheric drag. This force very slowly circularizes the orbits and the altitude is reduced too. The rate of decay of these orbits becomes extremely rapid at altitudes below 200 km. As soon as the satellite is down to 180 km it will only have a few hours to live and after several revolutions around the Earth it will re-entry down to Earth. Enhanced solar radiation at short wavelengths causes the upper atmosphere to expand and the drag on satellites in LEOs becomes larger.

[3] see also *http://www.ips.gov.au/Educational/1/3/7*

Table 7 Summary of geomagnetic indices

aa	3-hour range index, derived from two antipodal stations
AE, AU, AL	1- , 2.5-minute, or hourly auroral electrojet indices
am, an, as	3-hour range (mondial, northern, southern) indices
Ap	3-hour range planetary index derived from Kp
C, Ci, C9	Daily local (C) or international (Ci) magnetic character; C9 was first derived from Ci, then from Cp
Cp	Daily magnetic character derived from Kp
Dst	Hourly index mainly related to the ring current
K	3-hour local quasi-logarithmic index
Km	3-hour mean index derived from an average of K indices (not to be confused with the Km of the next item)
Km, Kn, Ks	3-hour quasi-logarithmic (mondial, northern, southern) indices derived from am, an, as
Kp, Ks	3-hour quasi-logarithmic planetary index and the intermediate standardized indices from which Kp is derived (not to be confused with the Ks of the preceding item)
Kw, Kr	3-hour quasi-logarithmic worldwide index and the intermediate from which Kw is derived
Q	Quarter hourly index
R	1-hour range index
RX, RY, RZ	Daily ranges in the field components
sn, ss	3-hour indices associated with an and as
U, u	Daily and monthly indices mainly related to the ring current
W	Monthly wave radiation index

Solar activity also influences on solar panels. The most efficient solar panels are the DS1 solar panels which convert about 22 % of the available energy into electrical power. The solar panels lose about 1-2 % of their effectiveness per year. After a five year mission, the solar panels will still be making more than 90 % . The two major dangers are: (i) Shortwavelength radiation emitted during solar flares can damage the electronics inside the panels.(ii) Micrometeorites, which are tiny, gravel-sized bits of rock and other space junk floating in space can scratch or crack solar panels.

5.4 Some Examples of Space Weather Damage

The Solar Proton Event in August 1972: This event occurred between the manned Apollo 16 and 17 missions. Even inside of a spacecraft the astronauts would have absorbed a lethal dose of radiation within 10 hours after the onset of the event. At 6:20 UT an optical flare was observed on the Sun. At 13:00 UT the astronauts' allowable 30-day radiation exposure to skin and eyes was exceeded. At 14:00 the astronauts' allowable 30-day radiation exposure for blood forming organs and the yearly limit for eyes was exceeded. At 15:00 the yearly limit for skin was exceeded.

At 16:00 UT the yearly limit for blood forming organs and the career limit for eyes was exceeded. At 17:00 UT the career limit for skin was exceeded.
October 1989 event: a major power failure occurred at ground in Quebec; an astronaut on the Moon would have been exposed to a lethal dose (protection possible by lunar soil). Astronauts on board of Mir received the full year radiation dose within few hours (Table 4).
The Bastille Day Event: an extremely powerful solar flare occurred on 14 July 2000. An X5-class solar flare caused a so called S3 radiation storm on Earth and fifteen minutes after the outburst of the flare the ionosphere was bombarded with energetic protons. Such storms cause the following effects on satellites: single-event upsets, noise in imaging systems, permanent damage to exposed components/detectors, and decrease of solar panel currents. It can also expose air travellers at high latitudes to low levels of radiation, the equivalent of a brief chest x-ray (Table 6). Also a full halo coronal mass ejection was observed and $> 10^{10}$ t of plasma was ejected into space towards Earth at speeds between 1300 and 1800 km/s. As a consequence of the geomagnetic disturbances Aurorae could be seen even at El Paso, power companies reported on damage of a transform, GPS accuracy was degraded for several hours. The K_p-index was larger than 9.

Mesospheric temperatures were found to be increased by 200 K because of this event (Dymond *et al.*, 2005, Tsurutani *et al.*, 2005).

5.5 Geomagnetically induced currents

As we have discussed, the magnetic field of the Earth is compressed by the interacting with solar magnetic clouds and particles. The changing magnetic field induces currents in the Earth and these induced currents produce magnetic fields that again disturb the Earth's surface magnetic field. The magnitude of the induced currents and electrical fields depends on electrical conductivities of the different layers within the Earth. Magnetic variations with lower frequencies penetrate deeper.

To simulate such ground effects, the real time GIC (Geomagnetic induced currents) simulator is available at *http://www.spaceweather.gc.ca/gic_simulator_e.php*.

There are several damaging effects of GICs like enhanced corrosion and power-failures. We mention a few well documented examples:

- On 30 October 2003 50 000 customers in Southern Sweden had no electricity due to a power failure caused by a GIC .
- Research on historical geomagnetic storms can help to create a good data base for intense and super-intense magnetic storms. For the event on March 13, 1989 the Dst $= -640$ nT.
- evidence for a superstorm that occurred on Sep 1-2 1859 with a Dst $= -1760$. This event was observed as a white light flare by Carrington. Tsurutani *et al.*, 2006, described the Halloween 2003 solar flares and the Bastille day event in 2000 and resultant extreme ionospheric effects. The October 28, 2003 flare caused a 30%, increase in the local noon equatorial ionospheric column density

within 5 minutes. Interplanetary coronal mass ejection (ICME) electric fields acted with a delay (due to solar wind propagation) with the ionosphere and the total electron content was enhanced by a factor of 300 %.

Acknowledgements I want to cordially thank the organizers for inviting me to give the lectures and their kind hospitality.

References

Arnold, F.: 2006, *SScRev.*, **125**, 169
Aschwanden, M., 2002: *Space Science Reviews*, **101**, 1
Dymond, K. F., Budzien, S. A., McCoy, R. P., Crowley, G.: 2005, AGU Fall Meeting Abstr., Dec., A116
Fröhlich, C.: 2006, *SScRev.*, **125**, 53
Gopalswamy, N., Aguilar-Rodriguez, E., Yashiro, S., Nunes, S., Kaiser, M. L., Howard, R. A., 2005, *Journal of Geophysical Research*, **110**, 12
Hanslmeier, A., 2007: *The Sun and Space Weather*, ASSL 347, Springer
Hughes, M. K., Diaz, H. F., 1994, *The medieval warm period*, Proc. Workshop Tucson 1991
Mekaoui, S., Dewitte, S.: 2008, *Solar Phys.*, **247**, 203
Shen, C., Wang, Y., Ye, P., Zhao, X. P., Gui, B., Wang, S., 2007, *Astrophys. J.* , 670, 849
Svensmark, H.; Friis-Christensen, E., 1997, *Atmos. Sol.-Terr. Phys.*, **59**, 11, 1225 - 1232
Tsurutani, B.T., Mannucci, A.J., Iijima, B., Guarnieri, F.L., Gonzalez, W.D., Judge, D.L., Gangopadhyay, P., Pap, J., 2006, *Advances in Space Research*, **37**, 1583-1588
Tsurutani, B.T., Judge, D.L., Guarnieri, F.L., Gangopadhyay, P., Jones, A.R., Nuttall, J., Zambon, G.A., Didkovsky, L., Mannucci, A.J., Iijima, B., Meier, R.R., Immel, T.J., Woods, T.N., Prasad, S., Floyd, L., Huba, J., Solomon, S.C., Straus, P., Viereck, R., 2005, *Geophys. Res. Lett.*, **32**, 3
Yermolaev, Yu.I., Yermolaev, M.Yu., Zastenker, G.N., Zelenyi, L.M., Petrukovich, A.A., Sauvaud, J.-A., 2005, *Planetary and Space Science*, **53**, 189-196